Effect of strong localization of doped holes in angle-resolved photoemission spectra of $La_{1-x}Sr_xFeO_3$

H. Wadati,[1] A. Chikamatsu,[2] M. Takizawa,[1] R. Hashimoto,[2] H. Kumigashira,[2] T. Yoshida,[1] T. Mizokawa,[1] A. Fujimori,[1] M. Oshima,[2] M. Lippmaa,[3] M. Kawasaki,[4] and H. Koinuma[5]

[1]*Department of Physics and Department of Complexity Science and Engineering, University of Tokyo, Kashiwa, Chiba 277-8561, Japan*
[2]*Department of Applied Chemistry, University of Tokyo, Bunkyo-ku, Tokyo 113-8656, Japan*
[3]*Institute for Solid State Physics, University of Tokyo, Kashiwa, Chiba 277-8581, Japan*
[4]*Institute for Materials Research, Tohoku University, 2-1-1 Katahira, Aoba, Sendai 980-8577, Japan*
[5]*National Institute for Materials Science, 1-2-1 Sengen, Tsukuba 305-0047, Japan*

(Dated: February 6, 2008)

We have performed an angle-resolved photoemission spectroscopy study of $La_{0.6}Sr_{0.4}FeO_3$ using *in situ* prepared thin films and determined its band structure. The experimental band dispersions could be well explained by an empirical band structure assuming the G-type antiferromagnetic state. However, the Fe 3*d* bands were found to be shifted downward relative to the Fermi level (E_F) by ~ 1 eV compared with the calculation and to form a (pseudo)gap of ~ 1 eV at E_F. We attribute this observation to a strong localization effect of doped holes due to polaron formation.

PACS numbers: 71.28.+d, 71.30.+h, 79.60.Dp, 73.61.-r

Metal-insulator (MI) transitions in strongly-correlated electron systems have been generally understood in terms of band-width control and filling control [1]. However, the actual situation is more complicated because of the effect of disorder, electron-phonon interaction, charge and orbital ordering, etc [2, 3, 4, 5, 6]. Electron-phonon interaction causes a polaronic effect on charge carriers and increases their effective masses. In some filling-controlled systems, carriers doped into the Mott insulator remain localized as self-trapped small polarons and the system remains insulating. The problem of how an MI transition occurs when strong electron-phonon interaction is present remains highly controversial. A striking example is a hole-doped Mott insulator (charge-transfer-type insulator) $La_{1-x}Sr_xFeO_3$ (LSFO), where the insulating phase is unusually wide in the phase diagram ($0 < x < 0.5$ at room temperature and $0 < x < 0.7$ at low temperatures) [7]. In a previous photoemission study, the gap at the Fermi level (E_F) was seen for all compositions in the range $0 \leq x \leq 0.67$ [8], consistent with the wide insulating region.

The effect of electron-phonon interaction is clearly reflected on the spectral function [9], and recent photoemission results have been discussed in this context for high-T_c superconductors [2, 3], Mn oxides [4], VO_2 [5], and Fe_3O_4 [6]. Angle-resolved photoemission spectroscopy (ARPES) is a particularly powerful technique by which one can directly study the band structure of a material. However, there have been few studies on transition metal oxides (TMOs) with the cubic perovskite structures like LSFO because many of them do not have a cleavage plane. Recently, the band structure of the three-dimensional perovskite $La_{1-x}Sr_xMnO_3$ has been studied by ARPES using well-defined surfaces of *in situ* prepared epitaxial thin films [10, 11], demonstrating that such an approach on TMO films is one of the best methods for such a purpose. In this paper, we report on *in-situ* ARPES results of single-crystal LSFO ($x = 0.4$) thin films grown on $SrTiO_3$ (001) substrates. We observed several dispersive bands which can be assigned to the Fe 3*d* e_g, t_{2g} and O 2*p* bands. The experimental band structure was interpreted based on an empirical tight-binding band structure assuming the G-type antiferromagnetic (AF) state. In spite of the overall agreement between experiment and theory, fundamental discrepancies were found for the overall shift of the Fe 3*d* bands away from E_F and the suppression of spectral weight around E_F. We shall discuss these discrepancies in terms of strong polaronic effect.

Experiment was carried out using a photoemission spectroscopy (PES) system combined with a laser molecular beam epitaxy (MBE) chamber at beamline BL-1C of the Photon Factory, KEK [12]. The LSFO ($x = 0.4$) thin films were grown epitaxially on Nb-doped $SrTiO_3$ substrates by the pulsed laser deposition method. Details are described in Ref. [8]. The lattice constants were determined to be $a = b = 3.905$ Å and $c = 3.883$ Å. In this paper, $k_\parallel$ denotes the in-plane electron momentum, and k_z the out-of-plane one, expressed in units of π/a or π/c. By low energy electron diffraction, sharp 1 1 spots were observed with no sign of surface reconstruction. ARPES measurements were performed under ultrahigh vacuum of $\sim 10^{-10}$ Torr at 150 K, below the Néel temperature ($T_N = 320$ K) of LSFO with $x = 0.4$ [7], using a Scienta SES-100 electron energy analyzer. The total energy resolution was set to about 150 meV. The E_F position was determined by measuring gold spectra.

Figure 1 shows ARPES spectra of an LSFO ($x = 0.4$) thin film taken with a photon energy of 74 eV. The inset shows a trace in k-space for $h\nu = 74$ eV with changing polar emission angle θ. Here, we have assumed the work function of the sample $\phi = 4.5$ eV, and the inner potential $V_0 = 10.5$ eV so that the periodicity of the band dispersion is correctly given in normal emission (not shown).

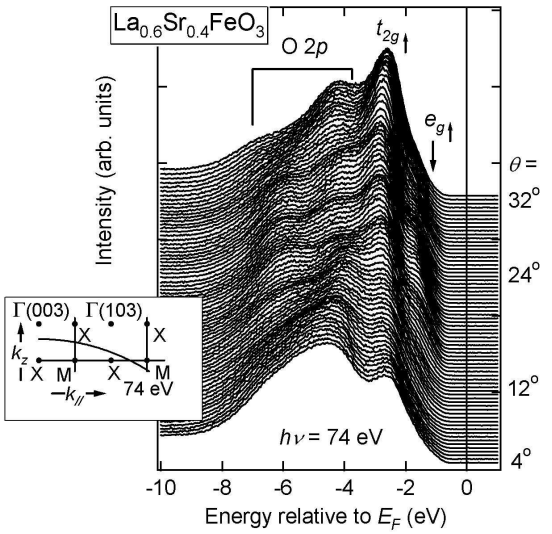

FIG. 1: ARPES spectra of an LSFO ($x = 0.4$) thin film taken at $h\nu = 74$ eV. Polar angle (θ) referenced to the surface normal is indicated. The inset shows the trace in k-space.

The shoulder structure at ~ -1.3 eV shows a significant dispersion, and is assigned to the Fe $3d$ majority-spin e_g bands. The peak structure at ~ -2.4 eV shows a weaker dispersion, and is assigned to the Fe $3d$ t_{2g} majority-spin bands. The structures at $-(4-7)$ eV show strong angular dependence and are assigned to O $2p$ bands. The e_g bands do not cross E_F, consistent with the insulating behavior and the persistence of the gap observed in the angle-integrated PES (AIPES) spectra [8].

The band dispersions are more clearly seen in the gray-scale plot in the left panel of Fig. 2 (a). Here, the second derivatives of the energy distribution curves (EDCs) are plotted on the gray scale with dark parts corresponding to energy bands. The same plot for $h\nu = 88$ eV [corresponding to the upper trace in Fig. 2 (c)] is shown in the left panel of Fig. 2 (b). In Fig. 2 (c), hole pockets obtained by the tight-binding calculation (described below) are also shown. The trace for 74 eV crosses the calculated hole pocket at $k_\parallel \sim 1.5\pi/a$, while that for 88 eV does not in the same $k_\parallel$ region. Figure 3 shows enlarged gray-scale plots near E_F in E-k space. Panel (a) is a direct intensity plot of the EDCs in Fig. 1. Angle-independent part has been subtracted as a background. Second derivatives of the EDCs are produced in panel (b) and those of momentum distribution curves (MDCs) in panel (c). In all the plots, the band has a minimum at $k_\parallel \sim 2.0\pi/a$, and disperses upward toward both sides and disappears at $k_\parallel \sim 1.5\pi/a$ and $k_\parallel \sim 2.5\pi/a$, not at E_F but ~ 1 eV below it.

In order to interpret the experimental band dispersions more quantitatively, we performed a tight-binding band-structure calculation with empirical parameters, following the scheme in Refs. [13, 14, 15]. We performed the calculation, however, assuming the G-type AF state cor-

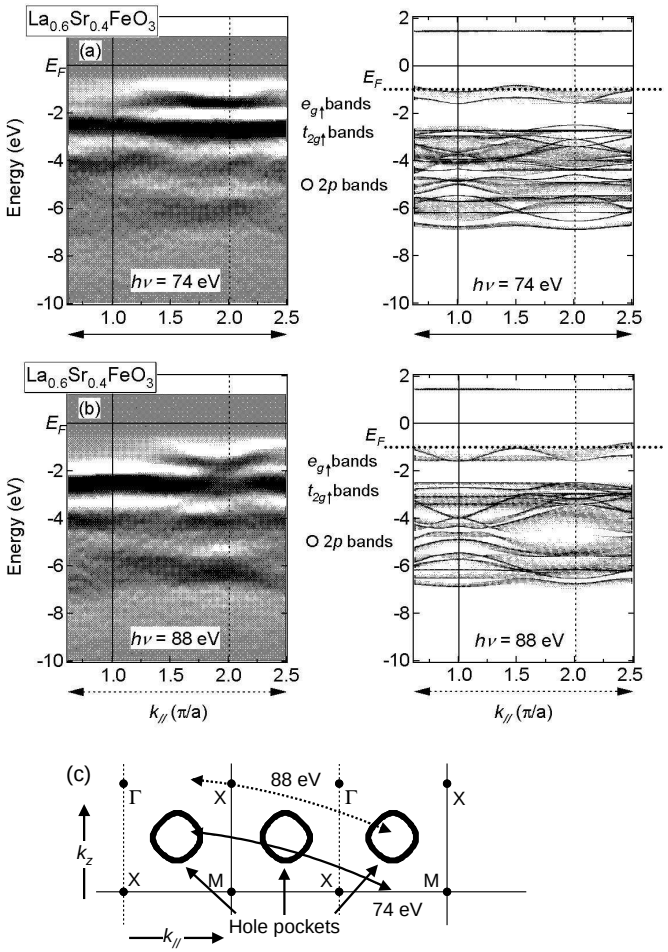

FIG. 2: Comparison of the ARPES spectra of LSFO taken at 74 eV (a) and 88 eV (b) with tight-binding calculation. The left panels show the experimental band structure deduced from the second derivatives of the EDCs (dark parts correspond to energy bands) and the right panels show the result of tight-binding calculation, taking into account the finite photoelectron mean-free path. The traces in k-space and calculated hole pockets are shown in (c).

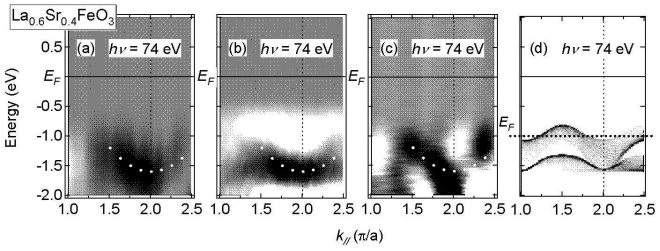

FIG. 3: Enlarged plot of ARPES spectra near E_F in E-k space. Panel (a): Intensity plot of the EDCs. Angle-independent part has been subtracted as a background. (b): Second derivatives of the EDCs. (c): Second derivatives of the MDCs. (d): Result of tight-binding calculation. White dotted curves are the guide to the eye.

responding to the magnetic ordering in LSFO. Here, the effect of G-type antiferromagnetism was taken into account phenomenologically by imposing an energy difference ΔE between the spin-up and spin-down Fe sites. Parameters to be fitted were therefore ΔE, the energy difference between the Fe $3d$ level and the O $2p$ level, $\epsilon_p - \epsilon_d$, and a Slater-Koster parameter, $(pd\sigma)$ [16]. For the other Slater-Koster parameters, we assumed $(pd\sigma)/(pd\pi) = -2.2$ [17, 18], and $(pp\sigma)$ and $(pp\pi)$ were taken to be 0.60 eV and -0.15 eV, respectively [18]. $(pd\sigma)$ is expected in the range of $-(1.4 - 1.9)$ eV from a configuration-interaction (CI) cluster-model calculation [8, 19]. Crystal-field splitting $10Dq$ of 0.41 eV was taken from Ref. [8]. It should be noted that $\epsilon_p - \epsilon_d$, $(pd\sigma)$ and ΔE primarily determine the Fe $3d$ − O $2p$ band positions, their dispersions, and the optical band gap, respectively, and therefore can be rather uniquely determined.

The best fit to the observed band dispersions of LSFO and the optical gap 2.1 eV of $LaFeO_3$ (LFO) [20] as shown in the right panels of Fig. 2 (a) and (b) has been obtained for reasoanble parameter values $\epsilon_p - \epsilon_d = 0$ eV, $(pd\sigma) = -1.5$ eV, and $\Delta E = 5.3$ eV. For these plots, we have considered the effect of k_z broadening (Δk_z) caused by a finite escape depth λ of photoelectrons [21] [$\Delta k_z \sim 1/\lambda$ (~ 0.2 Å^{-1}) is approximately 10 % of the Brillouin zone $(2\pi/c)$]. The dispersions of the e_g bands were thus successfully reproduced. The weak dispersions of the t_{2g} bands and the width of the O $2p$ bands were also well reproduced by these parameters. According to the band-structure calculation, spectral weight should be cut off above the calculated E_F, which is determined by the band filling for $x = 0.4$, while in experiment it gradually decreases from the calculated E_F toward the experimental E_F. This discrepancy inevitably arises from the fact that this material is insulating up to 70 % hole doping while the rigid-band model based on the present band strucure gives the metallic state.

Figure 4 (a) shows the density of states (DOS) of the G-type AF state calculated using the same parameter set. The partial DOS's for the majority-spin Fe e_g, the majority-spin t_{2g}, the minority-spin e_g, and the minority-spin t_{2g} orbitals are shown in the lower panels. A large band gap opens between the occupied majority-spin e_g bands and the unoccupied minority-spin t_{2g} bands for the present ΔE value. These characteristic features were already reported by the previous Hartree-Fock calculation [22] and the local spin-density-approximation calculation [23]. In Figs. 2 and 4, E_F for $x = 0.4$ has been determined from the filling of electrons when holes are doped into the AF insulator. In Figs. 4 (b) and (c) the calculated results are compared with the combined AIPES and O $1s$ x-ray absorption (XAS) spectra of LFO and LSFO ($x = 0.4$), respectively [8]. For LFO, the three main structures of the valance band, A, B, and C are successfully reproduced by the calculation, while the satellite structure in the valence-band photoemission spectrum could not be reproduced. The crystal-field splitting into D and E above E_F is also well reproduced. For LFO, although the

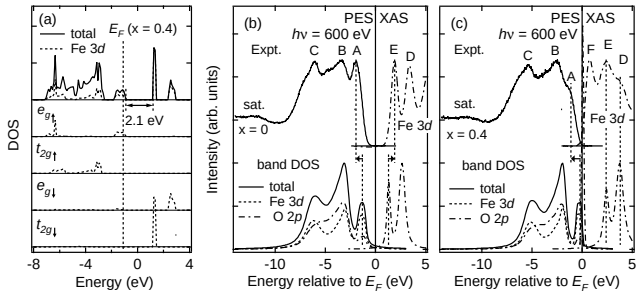

FIG. 4: Density of states obtained by using tight-binding calculation (a) and its comparison with the PES and O $1s$ XAS spectra of LFO (b) and LSFO ($x = 0.4$) (c) taken from Ref. [8].

calculated band gap has been adjusted to the experimental value, the peak positions of structures A and E are still shifted away from E_F in the experiment compared to the calculation [as denoted by broken lines in Fig. 4 (b)]. As for $x = 0.4$ [Fig. 4 (c)], strucure A is shifted away from E_F compared to the calculation even more.

Generally speaking, doped holes may be localized due to disorder or through coupling to lattice distortion. The latter effect, namely, polaronic effect was recently observed in the photoemission spectra of a number of TMOs [2, 4, 5, 6]. Note that for $x = 0.4$ a hole-induced peak F appears within the band gap of LFO and accomodates doped holes. These observations cannot be explained by the rigid-band model in which E_F has been shifted according to the band filling. The breakdown of the rigid-band model means that doped holes do not enter the top of the e_g majority-spin band but enter localized states split off from the top of the e_g band, causing the insulating behavior of this material.

Finally, we further discuss the discrepancy between the band-structure calculation and the experimental results near E_F and the origin of the insulating behavior of LSFO. Figure 5 schematically shows the calculated and experimental band structure and DOS of LSFO. Our tight-binding calculation is similar to local-density approximation (LDA) $+U$ in the sense that the effect of electron-electron interaction and hence the value of the band gap is adjusted via ΔE in the tight-binding calculation and via U in the LDA $+U$ calculation. Broken lines indicate the tight-binding or LDA $+U$ band structure, where the value of the band gap of the parent insulator has been adjusted to ~ 2 eV in order to reproduce the optical gap [20]. When holes are doped into this system, E_F moves downward and crosses the $e_{g\uparrow}$ band, making the system metallic if the rigid-band model can be applied. However, from the comparison of calculation and experiment in Figs. 2 and 4, the $e_{g\uparrow}$ structures are shifted away from E_F, and hole-induced states appear above E_F. The existence of these hole-induced states means that the rigid-band model is no more valid, and doped holes enter split-off localized states formed by

hole doping. There is also a spectral line-shape broadening compared to the band-structure calculation. Such a modification of the structures and line-shape broadening have been attributed to a polaronic effect recently observed in a number of TMOs [2, 5, 6]. For example, in the case of $Ca_{2-x}Na_xCuO_2Cl_2$, the spectral weight of quasiparticle peak Z becomes extremely small due to a strong coupling to phonons [2]. In the case of VO_2 [5] and Fe_3O_4 [6], spectral changes with temperature were interpreted by considering strong coupling of electrons to phonons. In the case of LSFO, we consider that electron-phonon coupling is strong enough to make Z almost zero (an insulating behavior), and shift the spectral features away from E_F. Since electron-phonon coupling is very strong for the e_g orbitals compared to the t_{2g} orbitals, the effect can be dramatic as observed in LSFO, where doped holes have e_g character. Moreover, according to the temperature-dependent PES and XAS studies, short-range (local) charge order may exist in the wide composition range [24]. The polaronic effect probably enhances the tendency toward local charge ordering and explains the unusually wide insulating phase in LSFO.

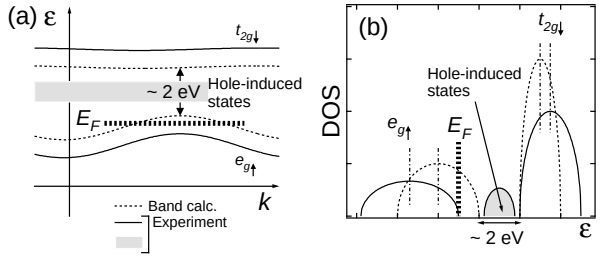

FIG. 5: Schematic picture of polaronic effects and hole-induced states in LSFO. (a) Band dispersions, (b) DOS.

In summary, we have performed an *in-situ* ARPES study on single-crystal LSFO ($x = 0.4$) thin films and determined its band structure. The observed dispersive bands were assigned to Fe $3d$ e_g, t_{2g} and O $2p$ bands. The experimental band dispersions were interpreted using a tight-binding band-structure calculation by assuming the G-type antiferromagnetic state. From the discrepancy near E_F between experiment and theory in spite of the overall agreement, the insulating behavior of this material is proposed to be caused by the localization of hole-induced states due to polaronic effect and/or short-range charge order.

The authors would like to thank N. Hamada and T. Saha Dasgupta for informative discussion and D. Kobayashi for sample preparation. We are also grateful to K. Ono for their support at KEK-PF. This work was supported by a Grant-in-Aid for Scientific Research (A16204024) from the Japan Society for the Promotion of Science (JSPS). This work was done under the approval of the Photon Factory Program Advisory Committee (Proposal No. 2002S2-002). H. W. acknowledges financial support from JSPS.

[1] M. Imada, A. Fujimori, and Y. Tokura, Rev. Mod. Phys. **70**, 1039 (1998).
[2] K. M. Shen, F. Ronning, D. H. Lu, W. S. Lee, N. J. C. Ingle, W. Meevasana, F. Baumberger, A. Damascelli, N. P. Armitage, L. L. Miller, Y. Kohsaka, M. Azuma, M. Takano, H. Takagi, and Z.-X. Shen, Phys. Rev. Lett. **93**, 267002 (2004).
[3] O. Rösch, O. Gunnarsson, X. J. Zhou, T. Yoshida, T. Sasagawa, A. Fujimori, Z. Hussain, Z.-X. Shen, and S. Uchida, Phys. Rev. Lett. **95**, 227002 (2005).
[4] N. Mannella, W. Yang, X. J. Zhou, H. Zheng, J. F. Mitchell, J. Zaanen, T. P. Devereaux, N. Nagaosa, Z. Hussain, and Z.-X. Shen, Nature (London) **438**, 474 (2005).
[5] K. Okazaki, H. Wadati, A. Fujimori, M. Onoda, Y. Muraoka, and Z. Hiroi, Phys. Rev. B **69**, 165104 (2004).
[6] D. Schrupp, M. Sing, M. Tsunekawa, H. Fujiwara, S. Kasai, A. Sekiyama, S. Suga, T. Muro, V. A. M. Brabers, and R. Claessen, Europhys. Lett. **70 (6)**, 789 (2005).
[7] J. Matsuno, T. Mizokawa, A. Fujimori, K. Mamiya, Y. Takeda, S. Kawasaki, and M. Takano, Phys. Rev. B **60**, 4605 (1999).
[8] H. Wadati, D. Kobayashi, H. Kumigashira, K. Okazaki, T. Mizokawa, A. Fujimori, K. Horiba, M. Oshima, N. Hamada, M. Lippmaa, M. Kawasaki, and H. Koinuma, Phys. Rev. B **71**, 035108 (2005).
[9] G. D. Mahan, *Many-Particle Physics* (Plenum, New York, 2003).
[10] M. Shi, M. C. Falub, P. R. Willmott, J. Krempasky, R. Herger, K. Hricovini, and L. Patthey, Phys. Rev. B **70**, 140407(R) (2004).
[11] A. Chikamatsu, H. Wadati, H. Kumigashira, M. Oshima, A. Fujimori, N. Hamada, T. Ohnishi, M. Lippmaa, K. Ono, M. Kawasaki, and H. Koinuma, cond-mat/0503373, Phys. Rev. B in press.
[12] K. Horiba, H. Oguchi, H. Kumigashira, M. Oshima, K. Ono, N. Nakagawa, M. Lippmaa, M. Kawasaki, and H. Koinuma, Rev. Sci. Instr. **74**, 3406 (2003).

[13] A. H. Kahn and A. J. Leyendecker, Phys. Rev. **135**, A1321 (1964).
[14] L. F. Mattheiss, Phys. Rev. **181**, 987 (1969).
[15] L. F. Mattheiss, Phys. Rev. B **6**, 4718 (1972).
[16] J. C. Slater and G. F. Koster, Phys. Rev. **94**, 1498 (1954).
[17] W. A. Harrison, *Electronic Structure and the Properties of Solids* (Dover, New York, 1989).
[18] L. F. Mattheiss, Phys. Rev. B **5**, 290 (1972).
[19] A. E. Bocquet, A. Fujimori, T. Mizokawa, T. Saitoh, H. Namatame, S. Suga, N. Kimizuka, Y. Takeda, and M. Takano, Phys. Rev. B **45**, 1561 (1992).
[20] T. Arima, Y. Tokura, and J. B. Torrance, Phys. Rev. B **48**, 17006 (1993).
[21] The effect of k_z broadening is given by the following Lorentzian function, $L(k_z) = 1/\{(k_z - k_{z0})^2 + (1/2\lambda)^2\}$, where λ denotes an escape depth of photoelectrons. Here we used the value $\lambda = 5$ Å.
[22] T. Mizokawa and A. Fujimori, Phys. Rev. B **54**, 5368 (1996).
[23] D. D. Sarma, N. Shanthi, S. R. Barman, N. Hamada, H. Sawada, and K. Terakura, Phys. Rev. Lett. **75**, 1126 (1995).
[24] H. Wadati, A. Chikamatsu, R. Hashimoto, M. Takizawa, H. Kumigashira, A. Fujimori, M. Oshima, M. Lippmaa, M. Kawasaki, and H. Koinuma, cond-mat/0410202, J. Phys. Soc. Jpn. in press.